



Review of Switched Beamforming Networks for Scannable Antenna Application towards Fifth Generation (5G) Technology

Nazleen Syahira Mohd Suhaimi¹, Nor Muzlifah Mahyuddin^{2*}

^{1,2}Universiti Sains Malaysia (USM)

School of Electrical and Electronic Engineering, Engineering Campus
14300 Nibong Tebal, Penang, MALAYSIA

*Corresponding Author

DOI: <https://doi.org/10.30880/ijie.2020.12.06.008>

Received 4 September 2019; Accepted 3 June 2020; Available online 2 July 2020

Abstract: The next generation wireless network (5G) addresses the evolution beyond mobile internet to massive Internet-of-Things (IoT) which will take off from 2019/2020 onwards. The essential design features in 5G wireless network system are massive multiple-input and multiple-output (MIMO) and steerable antenna array. The higher capacity, lower power transmission and larger system coverage offered by upcoming 5G technology can be realized using switched-beam antenna such as Butler matrix, Rotman lens, Blass matrix and Nolen matrix. Review of their design features and performance results will be compared in this article. Butler matrix can be the best approach owing to low complexity, orthogonal beams and less components utilization.

Keywords: Beamforming network, multi-beam, coupler, phase shifter, antenna array

1. Introduction

In today's digital era, wireless technology begins to view towards Fifth Generation (5G) with the concept on communication that unlimited between humans but additionally the machine-to-machine and vehicle-to-vehicle, which anticipated in the year beyond 2020 to fulfill higher-speed communication demand with very high data usage that increasing tremendously [1]. Furthermore, the exponential growth in demand for faster data rate and mobility of wireless applications has triggered the need for multimedia information towards 5G, which leads to the congested traffic of the data transfer. Another essential design features in a 5G wireless communication system is capability to fulfill the need of high data rate, efficient in usage of energy and cost, lower latency compared to fourth generation (4G) technologies and able to support a bigger number of operating devices. In addition to gratify the cost and experience demands, an extremely high security requirements, especially for services such as e-banking, safe driving, mobile health and security monitoring need to be fulfilled by 5G technology [2]. Moreover, 5G technology offers a lower power consumption to build a greener mobile communication network as well as to enhance terminal battery lifespan, explicitly for some IoT devices. Thus, numerous researches of wireless communication are studied to improve the communication in terms of data transfer speed, cost and its applications including the designs of antennas, wireless networks and IoT devices. The architecture of new 5G technology has a separated solution for indoor and outdoor applications. The distributed antenna system (DAS)

*Corresponding author: eemnmuzlifah@usm.my

architecture is applied particularly for indoor applications whilst massive multiple-input multiple-output (MIMO) architecture combined with steerable antenna array technologies used for outdoor applications [3]. Therefore, high-datarate and high-quality services to indoor users can be offered, whilst simultaneously lessening the pressure on outdoor applications. In order to support these 5G massive MIMO and steerable antenna array, a switched-beamforming network is required. However, it becomes a challenging task to utilize multiple antennas at the mobile terminal owing to compact

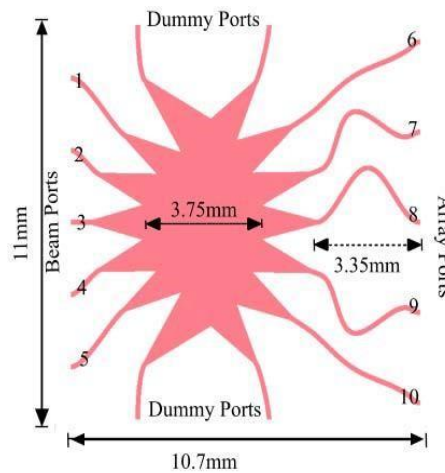


Fig. 1 - Layout design of Rotman lens geometry [4]

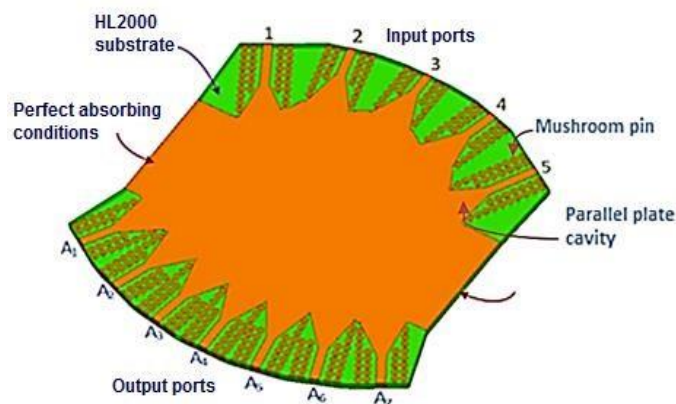


Fig. 2 - Ideal model of Rotman lens with ridge gap waveguides (RGW) [5]

in size of the terminal. The mutual coupling between the antenna elements increases while the distance between interelement spacing is too close. Various beams can be steered towards particular directions by applying smart antenna systems such as switched-beam antenna and adaptive array antenna. Although the switched-beam antenna and the adaptive array antenna consisting of a beamforming network which provides the multi-beams looking in various directions, the adaptive array antenna has more complex design and more pricey due to the presence of a sophisticated digital signal processing algorithm compared to the switched-beam antenna. Therefore, the beamforming network of the switched-beam antenna system is more attractive to be developed. These beamforming networks such as Rotman lens [410], [19], Butler matrix [11-13], [20], [23] Blass matrix [14], [15], [24], [25] and Nolen matrix [16], [17] are having different configurations that formed by commonly passive devices such as phase shifters, couplers and crossovers. Some research works regarding beamforming networks are reviewed in this article.

2. Beamforming Networks for Multi-Beam Antenna Applications

The switched-beam antenna develops multiple fixed beams with high sensitivity at the center of the beam and able to switch the main beam into the targeted direction by altering the phase differences of the signals to feed the antenna elements [18]. The review on the beamforming network is started with Rotman lens. In term of configuration design, the proposed work in [4] has been designed by integrating the Rotman lens and antenna array in low-temperature co-fired ceramic (LTCC) technology. The Rotman lens has been implemented based in ridge-gap waveguides (RGW) approach in which a metal ridge surrounded by a bed of mushroom pins guides the wave along a certain path to develop the waveguide in the air gap between the ridge and top metal plate, see Fig. 2. The 7 × 5 slotted antenna array is fed by the proposed RGW Rotman lens and its inter-element spacing is set to be 0.5 λ₀ in order to minimize the sidelobe level. In

this work, the return loss and isolation are better than 10 dB, whereas the mean measured insertion loss is $6 \text{ dB} \pm 1.6 \text{ dB}$ between 57 GHz and 66 GHz. At 60 GHz, the simulation results of the multi-beam antenna provide five beams (60° , 74° , 90° , 105° and 120°). The significance of this approach includes a low considerable loss.

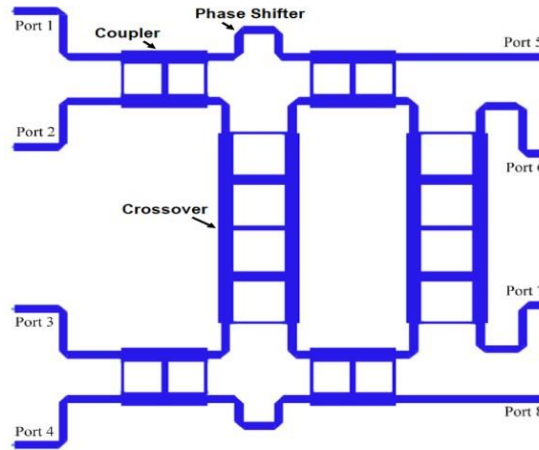


Fig. 3 - Topology of the proposed 4 x 4 Butler matrix network [11]

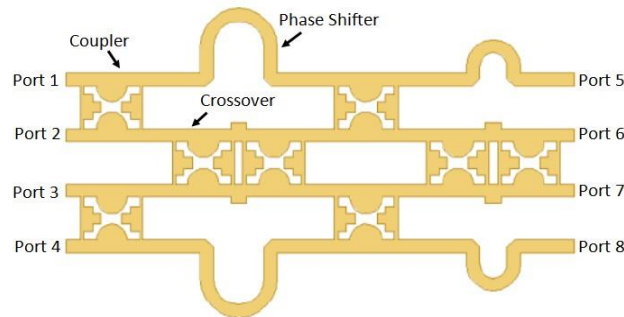


Fig. 4 - Layout of the proposed 4 x 4 miniaturized Butler matrix beamforming network [20]

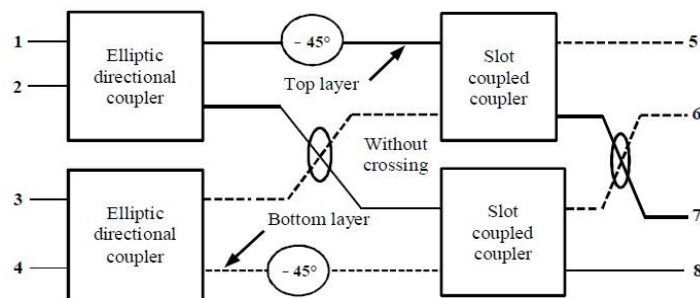


Fig. 5 – Block diagram of the two layers wideband 4 x 4 Butler matrix [21]

Despite this significant advantage, the performance can be degraded if the proposed design is fabricated and measured due to the misalignment and air gap between the multi-layer structures of ceramic substrates for the proposed Rotman lens with ridge gap waveguides. Even though the Rotman lens does not use any phase shifter and coupler, the phase error across the aperture still occurs unless fewer beam positions are chosen to obtain an excellent wavefront in the same direction. The high phase imbalance across the lens aperture limits the performance of the Rotman lens in [4] due to undesired reflection developed by geometry of the edge lens that nearby the star shaped transition on the array contour [19]. In order to minimize the phase error in Rotman lens, physical sizes of the focal length and lens are reduced as proposed in [5]. The proposed Rotman lens consists of five array ports, five beam ports, and absorbing materials that works as dummy ports as shown in Fig. 1. Rotman lens is integrated with antenna array using open ended $\lambda/4$ stubs to provide high gain, directivity, and wide bandwidth. The configuration design covers a small area, provides multiple beam directions and simple integration with the antenna. The maximum sidelobe level of this work is less than -12 dB due to high lens curvature and small degree of flare angle with medium sized of routed transmission lines.

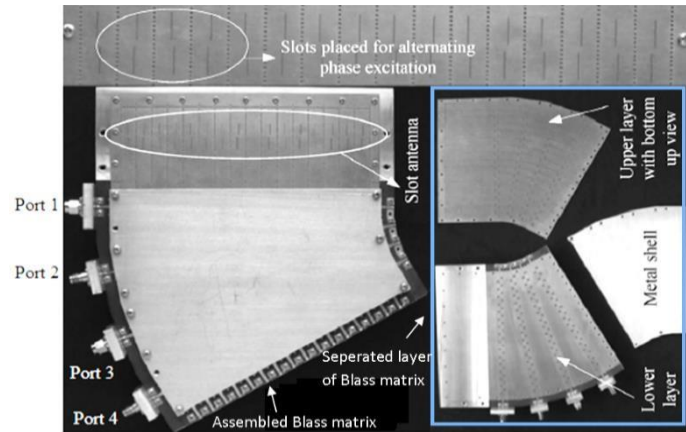


Fig. 6 - Photograph of the proposed SIW planar 4×16 Blass matrix [24]



Fig. 7 - Photograph of the modified two-beam Blass matrix [25]

The average insertion loss of all beam ports is less than 2.2 dB at the center frequency of 60 GHz. At 60 GHz, the simulated and measured insertion loss is less than 2.2 dB, whereas the return loss is less than -12 dB for each excited beam ports. Meanwhile, the simulated and measured coupling loss (S_{21} , S_{32} , S_{43} , and S_{54}) between adjacent beam ports of the Rotman lens are better than 10 dB between 50 GHz and 70 GHz. The proposed work needs a higher lens curvature to reduce the array factor sidelobes. Nevertheless, Rotman lens have many dummy ports which needs high cost of termination loads to be connected with the dummy ports. Another works of Rotman Lens are widely used as a beamforming technique in mm-wave applications [6-10]. According to the constraint on many termination loads are required by the Rotman lens which contribute to high cost, Butler matrix becomes a concern to form multi-beams.

The Butler matrix is developed by integrating the couplers, phase shifters and crossovers as presented in [11]. Fig. 3 shows a Butler matrix that composed of four two-section branch-line couplers and couplers, two 45° phase shifters and two four-section branch-line crossovers. The 10 dB bandwidth of simulated return loss for each excited port is 650 MHz at the central frequency of 2.4 GHz. Whilst, the isolation losses between input ports are better than 30 dB across frequency range between 2.01 GHz and 2.75 GHz. The simulated transmission coefficients are around -6 dB indicating equal power division of Port 1 between the output ports, except S_{51} and S_{61} which deteriorate slightly owing to the presence of coupling and phase errors in the four two-section branch-line couplers and two four-section branch-line crossovers. The simulated average errors of three phase differences between the output ports are around 6.12° . In order to reduce the size of the Butler matrix, the authors in [20] have miniaturized the 4×4 Butler matrix by using principle of impedance transformation method. This work consists of four miniaturized stepped hybrid couplers, two miniaturized stepped crossovers and two 45° meander line phase shifters. Theoretically, the phase gradient for input port 1 between the four output ports is -45° , whereas 135° for input port 2 at 2.4 GHz. The phase gradient excited by input ports 3 and 4 should be 45° and -135° owing to the symmetrical structure of the 4×4 Butler matrix topology. The transmission performance indicates the power is equally distributed from output port 5 to output port 8. The simulated error of the phase difference between the output ports while excited by input ports 1, 2, 3 and 4 is 5° , 7° , 7° and 5° , respectively. The amplitude fluctuation of the simulated output insertion loss is ± 1.8 dB at 2.4 GHz.

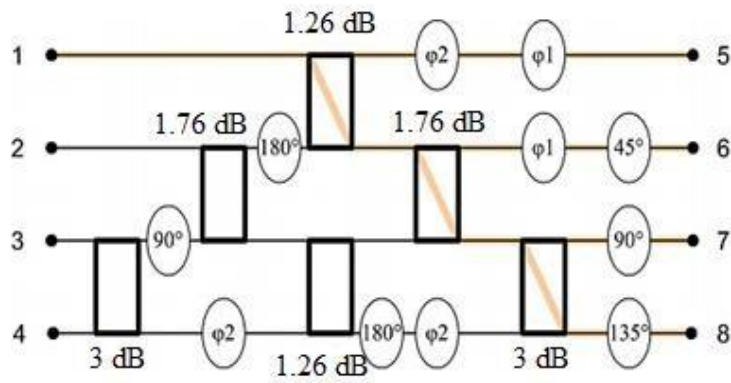


Fig. 8 - Block diagram of the proposed 4 x 4 Nolen Matrix based on coupler delay compensation of broadband substrate integrated waveguide (SIW) [16]

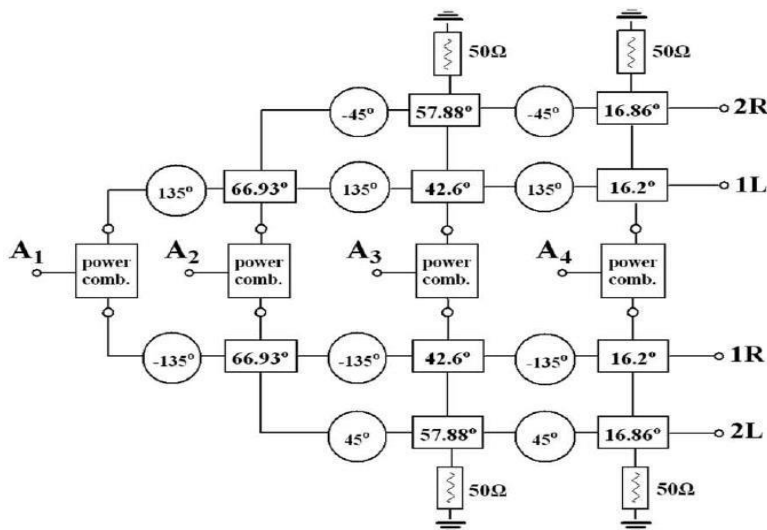


Fig. 9 - Photograph of the fabricated planar 4 x 4 Nolen matrix [17]

The performance of the miniaturized stepped 4 x 4 Butler matrix meets the design requirements. However, the presence of crossover in the proposed Butler matrix as developed in [11] and [20] will produce cross-coupling as well as mismatch loss. In order to eliminate the crossovers in the Butler matrix design, another simpler design of the 4 x 4 Butler matrix with no crossovers is presented in [21] using multi-layer technique. The wideband Butler matrix composing two elliptical directional couplers, two microstrip-slot coupled 3-dB couplers and two 45° phase shifters is depicted in Fig. 3. The simulated return loss is better than 10 dB between 1.6 GHz and 2.4 GHz. Meanwhile, deviation of the simulated insertion loss between port 1 and output ports is ± 0.5 dB. The main lobe can be pointed into four discrete orthogonal beams within $\pm 45^\circ$ (-45° , 15° , 15° and 45°) at 2.35 GHz.

Another concern beamforming network is Blass matrix. The Blass matrix in [15], [24], [25] does not require any crossovers and more flexible in deciding a standard number of input and output ports compared to the Butler matrix, which is restricted to be equal to the power of 2. In [15], the proposed 5×32 Blass matrix using the substrate integrated waveguide (SIW) technology consists of broad-narrow couplers and phase shifters is integrated with a phased antenna array to develop multi-beam directions. The phase deviation of the measured phase differences between output ports is $\pm 10^\circ$ across the frequency band. Five discrete beam directions of 30° , 35° , 40° , 45° and 50° are obtained at the center frequency of 11.575 GHz. This work provides efficiency about 65 % for each beam. Ohmic loss of 1.1 dB is occurred due to the height minimization of the feeding waveguides as well as to the input and output transitions. Another Blass matrix in [25] using the similar SIW technology as presented in the previous work in [15] is reported as shown in Fig. 6. The double layer planar 4 x 16 Blass matrix has 16 SIW cross slotted couplers with coupling values between 5.52 dB and 26 dB at each row of four input ports. The coupling factor range is varied by adjusting a cross-slot' length of the coupler. Meanwhile, arc angle of the phase shifter is set with equal spacing of 10° at the input ports to obtain the required phase shifting. The measured return loss responses are better than 10 dB from 15.125 GHz to 16.375 GHz when port 1 and port 2 are excited. The presence of termination loads at feeding line will reduce the efficiency to be 50% and causes fluctuation of the measured return loss at the remaining frequencies of port 1 and port 2. Moreover, the inherent loss of the Blass matrix is attributed to the resistive terminations will result in poor performance. The measured beam gains corresponding

to input port 1 to port 4 are 14.2 dB, 12.8 dB, 12.9 dB and 13.5 dB, respectively. Instead of realizing the SIW technology as reported in previous works [24], a single layer two-beam Blass matrix proposed in [25] is realized using the microstrip technology owing to its low-cost, ease of fabrication process and lightweight. As depicted in Fig. 7, the proposed Blass matrix has 7 phase shifters and 15 cascaded branch-line couplers which is used to achieve tight coupling values between -0.4 dB and -3.6 dB. The fabricated two-beam Blass matrix is verified between 5.3 GHz and 5.6 GHz. The measured return loss at each beam port shows better than 10 dB across the designated frequency band. Meanwhile, the main lobes of the proposed Blass matrix can be switched to 0° and 30° at 5.45 GHz. However, no latest work is found on Blass matrix due to the presence of inherent loss caused by the existence of termination loads at the end of feeding lines. Blass matrix provides low total efficiency owing to part of the signal in the Blass matrix flows into the terminated loads compared to the Butler matrix. In order to overcome this issue, the Blass matrix can be modified by replacing the diagonal couplers with some simple bent lines to construct the Nolen matrix.

The termination loads in the Blass matrix can be eliminated by implementing the Nolen matrix for beamforming applications. The Nolen matrix and Butler matrix can produce orthogonal beams due to its lossless characteristic in which only one beam reaches its peak amplitude of the main lobe, whereas other beams are located at a trough. The number of ports for the Nolen matrix can be flexible compared to the Butler matrix which requires a standard number of beam ports to be equal to a power of 2. A proposed Nolen matrix 4×4 Nolen matrix based on phase delay compensation at 77 GHz has been introduced in [16] as depicted in Fig. 8. The proposed 4×4 Nolen matrix is developed by interconnecting arbitrary coupling values of *H*-plane short-slot couplers such as 1.26 dB, 1.76 dB and 3 dB as well as phase shifters ranging from 0° and 180° . Moreover, some additional phase delay compensation of -15.7° and -53.2° are required in this work to satisfy wideband performances across the entire frequency band between 72 GHz and 82 GHz. The simulated and measured return loss and isolation are better than 10 dB across the frequency band. Whilst, amplitude deviation of the simulated and measured transmission coefficients are ± 1 dB and ± 3.5 dB between 73 GHz and 78 GHz when port 1 is excited, respectively. The simulated and measured transmission coefficients fluctuate around ± 1.8 dB and ± 4 dB, individually at the remaining frequencies due to the mismatch at each of the connectors for all ports and additional electrical path length of the phase delay compensations. The phase error between output ports (port 5 to port 8) across the entire frequency band is $\pm 12^\circ$ in the simulation, whereas $\pm 15^\circ$ in the measurement. Although the configuration of this matrix does not need any crossover as reported in [16] and [17], it consists of various distinct coupling values of couplers and phase shifters ranging from 45° to 180° which lead to higher complexity design. However, additional path loss will occur owing to the presence of additional phase delays which are required to achieve the desired beam directions. Another 4×4 Nolen matrix has been introduced in [17] as shown in Fig. 9 with different topology compared to work in [16]. This work is developed by interconnecting two 2×4 subnetwork consisting five two cascaded branch line couplers with arbitrary power divisions of 7.41 dB, 0.73 dB, 10.75 dB, 4.04 dB and 10.37 dB corresponding to various angle values, θ of 16.2° , 16.86° , 42.6° , 57.88° and 66.93° . It also consists of ten phase shifters ranging from -45° to 135° as well as four 3 dB Wilkinson power combiners, whereby the angles and phase of the couplers and phase shifters are determined by -30 dB Chebyshev distribution. The planar 4×4 Nolen matrix prototype is verified at center frequency of 3 GHz. The input return loss are better than 20 dB for about 150 MHz around the center frequency in simulation, whereas better than 15 dB for about 300 MHz around the center frequency in measurement. The worst case for deviation loss of the measured transmission coefficients is 2.5 dB compared to the simulated transmission coefficients. The worst side lobe level is -24 dB in simulation whereas -27 dB in measurement when input port 2R is excited at 3 GHz. This work provides four beam directions such as 15° , 45° , -15° and -45° when input ports 1R, 2R, 1L and 2L are excited, respectively. The review of the works in [4-5], [10-11], [16-17], [20-25] are compared and summarized in Table 1.

Table 1 - Qualitative review comparison of beamforming networks

Type of Networks	Works	Component Requirements	Advantage	Disadvantage beamforming
Rotman lens	[4-5]	Beam ports, a lens cavity, array ports and dummy ports	Low hardware components	Presence of mismatch loss and high cost due to the presence of termination loads at dummy ports and high phase imbalance across the lens aperture limits the performance owing to the undesired reflection caused by geometry of the edge lens.
	[10]	The desired phase front at the array input are obtained using path delay mechanism. A wideband circular patch L-shaped reflector antenna is connected with single layer Rotman lens to provide beam five scanning angles.	The path-length design mechanism in the microwave lenses Produce frequency independent beam steering, which considered as truetime delay (TTD) device and enhance the bandwidth of return loss.	Although the path lengths exhibit constant time-delay feature over the bandwidth, the lens is insensitive to the beam squint problems contributed by constant phase beamformers.
Butler matrix	[11], [20]	Couplers, phase shifters and crossovers	Low hardware components and low-cost	Presence of crossovers that contribute cross-coupling and mismatch loss.
	[21]	Couplers and phase shifters	No crossover	Presence of air gap due to misalignment of substrate layers limits the performance bandwidth.
	[22]	45° Couplers		Needs 45° output phase difference of couplers.
	[23]	30°, 120°, and 60° Couplers	No phase shifter and crossover	Needs flexible arbitrary output phase difference of couplers.
Blass matrix	[24], [25]	Cross couplers and phase shifters	Multiple beams capability placed in arbitrary directions and covering a broad scanning range	Compact designs that needs very tight coupling values of couplers, presence of mismatch loss and high cost due to the presence of termination loads at output ports as well as many hardware components with arbitrary number of beams with no limitations on their angular position are required.
Nolen matrix	[16]	Couplers and phase shifters		Presence of significant phase loss generated by unequal electrical paths connecting one input to every output.
	[17]	Couplers with arbitrary values of power divisions and angles as well as phase shifters with arbitrary values of phase	No crossover and flexible in deciding number of input and output ports	Various arbitrary coupling values of the couplers and arbitrary phase values of the phase shifters requirements as well as presence of significant phase loss introduced by the unequal electrical paths connecting one input to every output.

3. Conclusion

In conclusion, Butler matrix is the most suitable approach for beamforming scanning towards 5G since the planar realization of the Butler matrix is simpler with serial configuration of output ports and easier to be connected with the antenna array in order to develop switched-beam beamforming network. This configuration design is the most suitable approach for beamforming scanning towards 5G due to less hardware requirement, low-cost for fabrication and lightweight device, compact size and low power consumption since the power is transmitted towards the particular direction. Thus, the best configuration design of the beamforming networks to be selected is the Butler matrix.

Acknowledgement

This work is carried out with the financial support from the Universiti Sains Malaysia via Fundamental Research Grant Scheme (FRGS) (203.PELECT.6071373)

References

- [1] Hassani, S. E., & Haidine, A. (2015). Roadmap towards beyond 4G: Key technologies and challenges for 5G. International Conference on Wireless Networks and Mobile Communications (WINCOM), 1-6.
- [2] Liu, G., & Jiang, D. (2016). 5G: Vision and requirements for mobile communication system towards year 2020. Chinese Journal of Engineering, 1-8.
- [3] Wang, C.-X., Haider, F., Gao, X., You, X.-H., Yang, Y., Yuan, D., et al. (2014). Cellular architecture and key technologies for 5G wireless communication networks. IEEE Communications Magazine, 52(2), 122-130.
- [4] Attaran, A., Rashidzadeh, R., & Kouki, A. (2016). 60 GHz low phase error Rotman lens combined with wideband microstrip antenna array using LTCC technology. IEEE Transactions on Antennas and Propagation, 64(12), 5172-5180.
- [5] Carrera-Suarez, L. F., Navarro-Méndez, D. V., Baquero-Escudero, M., Valero-Nogueira, A. (2015). Rotman lens with ridge-gap waveguides, implemented in LTCC technology for 60 GHz applications. 9th European Conference on Antennas and Propagation (EuCAP), 1-5.
- [6] Pokorný, M., Säily, J., & Aurinsalo, J. (2013). Development of 60 GHz phased antenna array based on a Rotman lens. Rotman Lens Origin Interesting Properties of Rotman Lens Example RL Design at 50-70 GHz Difficulties in Practical Implementation. WICOMT of the operational program Education for Competitiveness.
- [7] Lee, W., Kim, J., Cho, C. S., & Yoon, Y. J. (2009). A 60 GHz rotman lens on a silicon wafer for system-on-a-chip and system-in-package applications. IEEE MTT-S Int. Microwave Symposium Digest. 1189-1192.
- [8] Lee, W., Kim, J. & Yoon, Y. J. Compact Two-Layer Rotman Lens-Fed Microstrip Antenna Array at 24 GHz. IEEE Transactions on Antennas and Propagation, 59(2), 460-466.
- [9] Hassanien, M. A., Jenning, M., & Plettemeier, D. (2016). Miniaturized beam steerable system using rotman lens for mm wave applications at 60GHz. 16th Mediterranean Microwave Symposium (MMS), 1-4.
- [10] Hassanien, M. A., Hahnel, R., & Plettemeier, D. (2018). A Novel Electronically Wideband Steering System using Rotman Lens for 5G Applications at 28 GHz. 12th European Conference on Antennas and Propagation (EuCAP), 1-5.
- [11] Nachouane, H., Najid, A., Tribak, A., & Riouch, F. (2014). Broadband 4×4 Butler matrix using wideband 90° hybrid couplers and crossovers for beamforming networks. International Conference on Multimedia Computing and Systems (ICMCS), 1444-1448.
- [12] Zaidel, D. N. A., Rahim, S. K. A., & Seman, N. (2015). 4×4 Ultra Wideband Butler Matrix for Switched Beam Array. Wireless Personal, 82(4).
- [13] Ausordin, S. F., Abdul Rahim, S. K., Seman, N., Dewan, R., & Sa'ad, B. (2013). A compact 4×4 butler matrix on double-layer substrate. Microwave and Optical Technology Letters, 56(1), 223-229.
- [14] Li, B., Chen, Y., Fu, Z., Chen, R. T. (2000). Substrate-guided wave optical true-time-delay feeding network for phased-array antenna steering. Proceedings of the International Society of Optics and Photonics (SPIE), 256-265.
- [15] Casini, F., Gatti, R. V., Marcaccioli, L., & Sorrentino, R. (2007). A novel design method for Blass matrix beamforming networks. Proceedings of the 37th European Microwave Conference, EuMA, 1512-1514.
- [16] Djerafi, T., Fonseca, N. J. G., & Wu, K. (2011). Broadband Substrate Integrated Waveguide 4×4 Nolen Matrix Based on Coupler Delay Compensation. IEEE Transactions on Microwave Theory and Techniques, 59(7), 1740-1745.
- [17] Fakoukakis, F. E., & Kyriacou, G. A. (2013). Novel Nolen matrix based beamforming networks for series-fed low SLL multibeam antennas. Progress in Electromagnetics Research, 51, 33-64.
- [18] Thomas, Jr. D. D. (2019). U.S. Patent No. 10,209,353 B2. North Syracuse, NY: U.S. Patent and Trademark Office.
- [19] Shahi, A., Mohammad-Taheri, M., & Aryanian, I. (2018). A 5G Multibeam Antenna Including Rotman Lens and Slot Array Antenna. Proceedings of the 5th International Conference on Millimeter-Wave and Terahertz Technologies (MMWaTT), 78-81.

- [20] Liang, R., Zhang, Y., Yan, W., Wang, J., Tong, Y., Lin, C., & Chang, Q. (2018). A Novel Design of Miniaturized Butler Matrix. 18th International Conference on Communication Technology (ICCT), 560-563.
- [21] Sfar, I., & Osman, L. (2016). Overview of wideband Butler matrix in microstrip-slot technology for beamforming antenna applications. 5th International Conference on Multimedia Computing and Systems (ICMCS).
- [22] Babale, S. A., Abdul Rahim, S. K., Barro, O. A., Himdi, M., & Khalily, M. (2018). Single layered 4 x 4 butler matrix without phase shifters and crossovers. *IEEE Access*, 6, 77289-77298.
- [23] Han, K., Li, W., & Liu, Y. (2019). Flexible phase difference of 4×4 Butler matrix without phase-shifters and crossovers. *International Journal of Antennas and Propagation*, 1-7.
- [24] Chen, P., Hong, W., Kuai, Z., & Xu, J. (2009). A Double Layer Substrate Integrated Waveguide Blass Matrix for Beamforming Applications. *IEEE Microwave and Wireless Components Letters*, 19(6), 374–376.
- [25] Lim, W. Y., & Chan, K. K. (2009). Generation of multiple simultaneous beams with a modified Blass matrix. *Asia Pacific Microwave Conference (APMC)*, 1557–1560